

Solar tower combined cycle plant with thermal storage: energy and exergy analyses

Soumitra Mukhopadhyay^a and Sudip Ghosh^{*}

Department of Mechanical Engineering, Indian Institute of Engineering Science and Technology,
Howrah 711103, West Bengal, India

(Received March 9, 2015, Revised December 25, 2015, Accepted January 7, 2016)

Abstract. There has been a growing interest in the recent time for the development of solar power tower plants, which are mainly used for utility scale power generation. Combined heat and power (CHP) is an efficient and clean approach to generate electric power and useful thermal energy from a single heat source. The waste heat from the topping Brayton cycle is utilized in the bottoming HRSG cycle for driving steam turbine and also to produce process steam so that efficiency of the cycle is increased. A thermal storage system is likely to add greater reliability to such plants, providing power even during non-peak sunshine hours. This paper presents a conceptual configuration of a solar power tower combined heat and power plant with a topping air Brayton cycle. A simple downstream Rankine cycle with a heat recovery steam generator (HRSG) and a process heater have been considered for integration with the solar Brayton cycle. The conventional GT combustion chamber is replaced with a solar receiver. The combined cycle has been analyzed using energy as well as exergy methods for a range of pressure ratio across the GT block. From the thermodynamic analysis, it is found that such an integrated system would give a maximum total power (2.37 MW) at a much lower pressure ratio (5) with an overall efficiency exceeding 27%. The solar receiver and heliostats are the main components responsible for exergy destruction. However, exergetic performance of the components is found to improve at higher pressure ratio of the GT block.

Keywords: brayton cycle; power tower; thermal storage; combined cycle; exergy analysis

1. Introduction

Fast increasing energy demand is associated with the increase of worldwide population and rapid social and industrial developments. The emissions from the conventional power plants are producing global warming, and deterioration of ozone layer (Reuss *et al.* 1997). This has become a pressing issue and needs to be tackled. The situation has forced researchers to look for more efficient ways of energy resources with a higher share of renewable energy options. Out of various renewable energy options available, solar energy has proved its worth in addressing the issue of environmental pollution and global warming. It is observed that around 51% of the total incoming solar radiation reaches the land and the oceans after attenuation by both the clouds and atmosphere

^{*}Corresponding author, Associate Professor, E-mail: sudipghosh.becollege@gmail.com

^aPh.D. Student, E-mail: soumitra1995@gmail.com

(Earth's Energy Budget 2014).

The power from the sun intercepted by the earth is approximately 1.8×10^{11} MW, which is many thousands of times larger than the present consumption rate on the earth of all commercial energy sources (Sukhatme and Nayak 2008). Solar thermal power has probably the greatest potential of any single renewable energy area (Mills 2004). Abengoa Yield, which is in the sustainable energy market, has established a 280 MW CSP plant located in California and the plant will provide clean electricity to 90,000 households in California (Solar Server Report 2015). For solar thermal applications, solar irradiation is absorbed by a solar collector as heat which is then transferred to its working fluid (air, water or oil). The heat carried by the working fluid can be used to either provide domestic hot water/heating, or for producing power. Low-temperature collectors are flat plates, generally used to heat swimming pools. Medium-temperature collectors are usually parabolic troughs but are used for heating water or air for residential and commercial use. For high temperature applications, parabolic dishes or Fresnel collectors are used and solar power tower is used for very high temperature applications, mainly for utility scale power plants. In solar power tower, which is also known as 'central tower' power plants or 'heliostat' power plants or power towers, is a type of solar furnace, where a solar receiver is mounted at the top of a tower to receive the focused sunlight. The sun's ray is focused by an array of flat, movable mirrors, called heliostats. Current central receiver systems are suited to electrical power outputs of 30 to 400 MWe.

One of the biggest challenges of the solar thermal based power plants is the intermittency of the source (Shabgard *et al.* 2012). However, using the highly efficient heat transfer properties of molten salt, this technology facilitates electricity production from weather volatility and, more importantly, it offers the capability to dispatch electricity while solar energy is not available. A thermal storage system provides an added benefit: allowing the plant to be designed to optimize the electricity load profile to meet specific market needs. The intermittency can be overcome by introducing thermal energy storage of molten salt and this can be integrated with the solar thermal power plants. In this case, excess thermal power is required to be generated at peak sun-shine hours that is later dispatched during periods of insufficient insolation. Among various thermal energy storage media available, thermal oils (like Therminol VP-1) and molten salts are used in commercial applications. Use of thermal oils is restricted due to its high cost, flammability, and temperature limitation (400°C) for which high thermodynamic efficiency of the power block

Table 1 Characteristics of some of the commercial salts and Therminol VP-1 (Kearney *et al.* 2003)

Property		Solar Salt	Hitec	Hitec XL(Calcium Nitrate Salt)	Therminol VP-1
Composition (%)	Sodium Nitrate	60	7	7	Diphenyl/biphenyl oxide
	Potassium Nitrate	40	53	45	
	Sodium Nitrite		40		
	Calcium Nitrite			48	
Freezing Point (°C)		220	142	120	13
Upper Temperature (°C)		600	535	500	400
Density @ 30°C in kg/m ³		1899	1640	1992	815
Viscosity @ 30°C		3.26	3.16	6.37	0.2
Heat capacity @ 30°C in kJ/kg-K		1.495	1.560	1.447	2.319

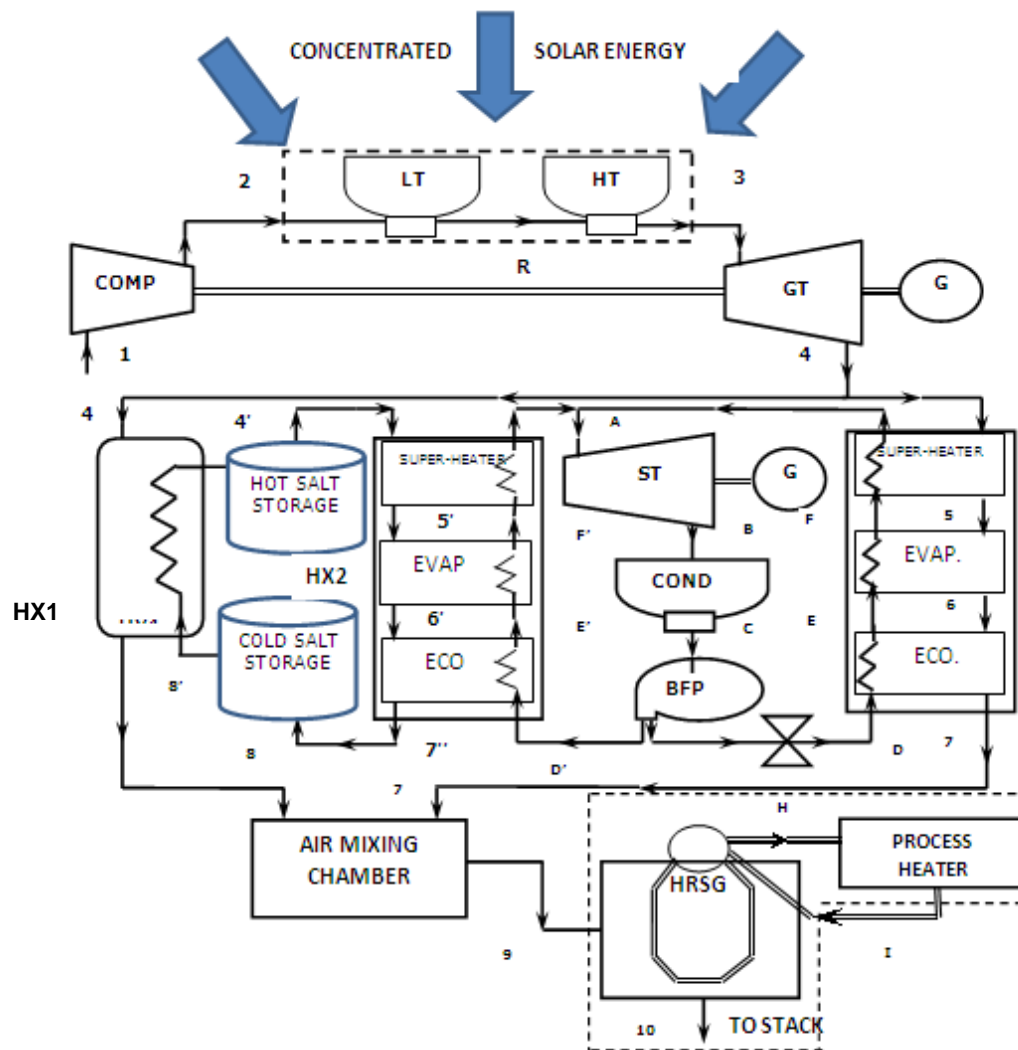


Fig. 1 Schematic of the proposed model

cannot be achieved (Flueckiger *et al.* 2013). On the other hand, molten salt is used in solar power tower systems because it is liquid at atmosphere pressure, it provides an efficient, low-cost medium, its operating temperature is compatible with today's high-pressure and high-temperature steam turbines, and it is non-flammable and nontoxic in nature. Characteristics of some of the commercial salts used in the solar thermal power plants and Therminol VP-1 are given in Table 1 (Kearney *et al.* 2003). Solar thermal systems using molten salts (40% potassium nitrate, 60% sodium nitrate) as the working fluids are now in operation. Montes *et al.* (2010) developed a thermo-fluiddynamic model for parabolic trough collectors with various working fluids like oil, molten salt, or water/steam. The influence of collector length, absorber tube diameter, working temperature, and pressure has been evaluated on energetic and exergetic performance. The paper concludes that that direct steam generation is more efficient than oil and molten salt systems.

In the present paper, solar power tower combined heat and power (CHP) cycle has been

proposed, using a solar receiver mounted at the top of the tower. Brayton cycle has been considered as the topping cycle with air as the working fluid. The exhaust air from the topping cycle has been used to generate power in a steam turbine generator as well as to produce process steam. The detailed thermodynamic analysis of the cycle has been carried out energetically as well as exergetically. Component wise exergy analysis has been done to identify the components where considerable exergy loss occurs.

2. Model description

Fig. 1 shows the schematic of a solar power towered gas turbine combined plant considered in the present study. Ambient air at point 1 (300K and 1.01325 bar pressure) enters the compressor (**COMP**) and leaves at point 2. Compressed air then enters the solar receiver (**R**) which raises the air temperature in two stages until a final temperature of 1000°C (1273 K) is achieved. Two stages of the solar receiver are: low temperature (**LT**), and high temperature (**HT**) modules. In the receiver cluster the air from the compressor of the gas turbine is heated up to 1000°C by concentrated solar energy. Fig. 2 shows a schematic of a solar concentrator-receiver system which traps the incoming solar flux into the working fluid in the receiver. A number of heliostats concentrate the solar radiation into the solar receivers, which are mounted on top of a tower. Heated air enters the gas turbine (**GT**) at point 3 and expands to point 4. The gas turbine module is similar in construction with the first prototype solar powered gas turbine system, installed during 2002 in the CESA-1 tower facility at Plataforma Solar de Almeria (PSA) in Spain (Heller *et al.* 2006), but of a larger scale.

A part of the exhaust from GT is passed through a HRSG to produce superheated steam which in turn will be utilized to run a steam turbine in the bottoming cycle. In the HRSG, air is first used to raise the temperature of the steam in the superheater (**SUP**) from point 'F' to the point 'A'. Then

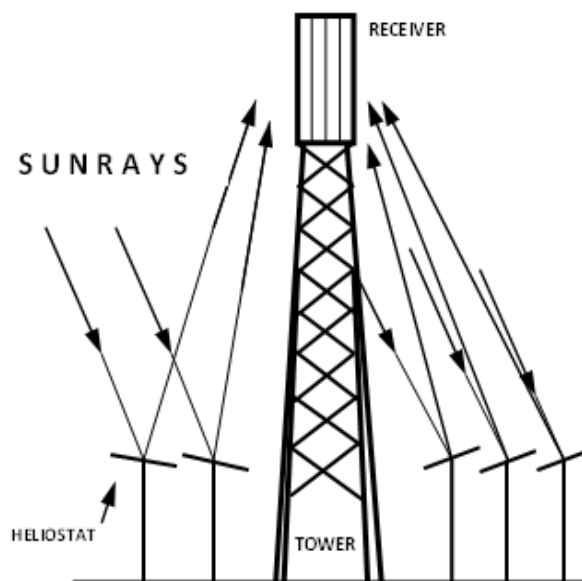


Fig. 2 Solar concentrator receiver system

the air is used to evaporate the water from point 'E' to 'F' in the evaporator (**EVAP**) and finally, it is utilized to heat the feed water in the economiser (**ECO**) i.e., to raise the temperature of the feed water to saturation temperature. The superheated steam at point 'A' (65 bar pressure and 460°C) enters into the steam turbine (**ST**), and after doing work in the steam turbine, steam is exhausted in the condenser (**COND**) at point 'B' at 0.075 bar pressure. After being condensed in the condenser, water is pumped from point 'C' to point 'D' i.e., at the boiler pressure by boiler feed pump (**BFP**). The system as well as the programming is developed in such a way that the temperature difference between the evaporator exit temperature of air (i.e., T_E) and the saturation temperature of water (i.e., $T_E=T_F$) does not fall below 15°C for better heat transfer.

The other part of the hot exhaust air from gas turbine is utilized to heat up the molten salt in the heat exchanger (**HX1**), and heats up the molten salt during the peak sun-shine hours, coming out from the cold salt storage tank, which acts as the storage medium. The hot salt coming from HX1 is stored in the hot salt storage tank. While sufficient sunlight is not available, the hot salt from the hot salt storage tank flows to another heat exchanger **HX2**, which comprises of economiser, evaporator and the superheater. HX2 produces superheated steam in the same condition as during the daytime (i.e., 65 bar, 460°C). The same steam turbine is used to generate the power for 4 hours at a power level equivalent to that of peak sun- shine hours. The minimum molten salt temperature at the exit of the economiser is restricted to 290°C to avoid freezing of the molten salt mixture.

The air stream at state points 7 and 8 are mixed in an air mixing chamber. Additional recoverable heat in the hot exhaust air is further utilized by raising saturated steam at low pressure (1.01325 bar) for use in a process plant.

2.1 Solar receiver model

The solar receiver considered here is having two modules: low and medium temperature modules. Both the modules are similar in construction as used in SOLGATE project. In SOLGATE project, the used low temperature (LT) module was nothing but a tubular receiver which consisted of parallel tubes (Heller *et al.* 2006). The outlet temperature of air from the LT module was 550°C. For the high temperature (HT) module, ceramic foam absorber was used, installed on a ceramic mounting structure, and the foam was coated with a silica layer.

3. Mathematical model descriptions of the system

Following assumptions are made for the simulation of the solar CHP plant:

- (a) Air has been considered as ideal gas. However, C_{pa} is assumed to be a polynomial function of temperature (Cengel and Boles 2003).
- (b) Mirror reflectivity has been considered as 90% (Xu *et al.* 2011).
- (c) No pressure loss takes place in any equipment or in air or steam paths except in the receiver where pressure drop has been considered as 120 mbar. Also, no extraneous heat loss occurs in any equipment.
- (d) Gas turbine inlet temperature of air is assumed as 27°C.
- (e) Steam turbine inlet temperature and pressure of superheated steam as 460°C and 65 bar.
- (f) Condenser pressure has been taken as 0.075 bar.
- (g) The molten salt at hot salt storage tank is kept at 565°C and salt at cold salt storage tank is at minimum 290°C (Flueckiger *et al.* 2014)

- (h) Specific heat of molten salt is 1.6 kJ/kg-K (Herrmann *et al.* 2002)
 (i) Air exit temperature to stack is assumed as 127°C (400 K).

3.1 Energy analysis

In this section, first law analysis or the energy analysis of the CHP plant has been carried out based on the following methodology.

3.1.1 Compressor and gas turbine

Initially, mass flow rate of air (m_a) is considered as 3 kg/s. Since temperature of air at the entry to the compressor and pressure ratio (r) is known, temperature after isentropic compression is given by the following equation

$$T_{2'} = T_1 (r)^{\frac{k-1}{k}} \quad (1)$$

But after actual compression in the compressor, temperature is obtained from the following equation considering isentropic efficiency of compression $\eta_c=0.88$

$$T_2 = T_1 + \frac{1}{\eta_c} (T_{2'} - T_1) \quad (2)$$

Similarly, considering the isentropic efficiency of expansion ($\eta_{e,GT}$) as 0.90, temperature after expansion from gas turbine is given by the following equation

$$T_4 = T_3 - \eta_{e,GT} (T_3 - T_{4'}) \quad (3)$$

3.1.2 HRSG

Initially, outlet temperature of air from economizer is considered as 120°C and later on it is corrected. Approximate mass flow rate of water (m_w) in the bottoming steam turbine plant can be found out from the overall energy balance in the heat recovery steam generator (HRSG) and the enthalpy (h) at different points. Approximate mass flow rate of water in HRSG can be calculated from the following equation

$$m_w = \frac{m_a \int_{T_7}^{T_4} C_{pa} dT}{(h_A - h_D)} \quad (4)$$

where C_{pa} is the specific heat of air which follows the following polynomial equation where a_0 , b , c , d are constants.

$$C_{pa} = a_0 + bT + cT^2 + dT^3 \quad (5)$$

In the superheater, steam is superheated by the hot exhaust air from the gas turbine. Evaporator inlet temperature of air (T_5) can be calculated from the energy balance equation in the superheater and is given by

$$T_5 = T_4 - \frac{m_w (h_A - h_F)}{m_a C_{pa}} \quad (6)$$

In the evaporator also, water is evaporated by taking the heat energy from air. Outlet temperature of air (T_6) from the evaporator can be calculated from the energy balance equation in evaporator

$$T_6 = T_5 - \frac{m_w (h_F - h_E)}{m_a C_{pa}} \quad (7)$$

For better heat transfer, T_6 should be 15°C more than the saturation temperature of water. If the calculated T_6 does not satisfy this condition, custom-made codes in 'C' are developed in such a way that m_w is reduced by 0.001 kg/s and T_6 is recalculated. The process is repeated until T_6 satisfies the above condition and finally corrected T_7 is calculated from the below energy balance equation in economiser

$$T_7 = T_6 - \frac{m_w (h_E - h_D)}{m_a C_{pa}} \quad (8)$$

Considering mechanical efficiency ($\eta_{mech.}$) as 0.95 and generator efficiency (η_G) as 0.97, net power obtained from steam turbine

$$(P_{net})_{ST} = (P_{ST} - P_{Pump}) \eta_{mech.} \eta_G \quad (9)$$

Thermal efficiency of the steam cycle

$$(\eta_{th})_{ST} = \frac{(P_{net})_{ST}}{m_w (h_A - h_D)} \quad (10)$$

3.1.3 Calculation for mass flow rate of salt in HX2

Thermal energy required to be stored in the salt storage to run steam turbine at the rated output for 4 hours when sunlight is not available is given by the following equation

$$EnergyStored = \frac{4 \times (P_{net})_{ST} \times 1000}{(\eta_{th})_{ST}} \quad (11)$$

Approximate mass flow rate of salt through the HX2 can be calculated from the following equation

$$m_{salt} = \frac{EnergyStored}{1.6 \times (838 - 563) \times 4 \times 3600} \quad (12)$$

where specific heat of molten salt is 1.6 kJ/kg-K; maximum and minimum temperatures of molten salt are 565°C (838 K) and 290°C (563 K).

Temperature of molten salt after superheater, evaporator and economiser can be found out from the energy balance equation in the corresponding component. The temperature of the molten salt is maintained between 290°C (563 K) and 565°C (838 K). If the temperature of the molten salt at the outlet of the economiser is less than 290°C, mass flow rate of molten salt is revised so that the outlet temperature is more than 290°C.

Amount of salt required to be stored to run the steam turbine for 4 hours during non-availability

of sun-light can be obtained from the below equation

$$M_{salt} = (4 \times 3600 \times m_{salt}) \quad (13)$$

Heat energy required to be stored in molten salt is given by

$$E_{salt} = \frac{M_{salt} \times C_{p-salt} \times (838 - 563)}{\eta_{storage}} \quad (14)$$

Considering 6 peak sun-shine hours, heat stored in salt per second is given by

$$e_{salt} = \frac{E_{salt}}{(6 \times 3600)} \quad (15)$$

So, additional air required to heat the salt to required temperature is given by the below equation

$$m_{a(Addl.)} = \frac{e_{salt}}{\eta_{effectiveness} \times \int_{563}^{T_4} C_{pa} dT} \quad (16)$$

Required incident solar energy on the heliostat field is obtained by dividing the required heat energy to heat the GT air by the product of heliostat field optical efficiency and the receiver efficiency.

$$Q = \frac{(m_a + m_{a(Addl.)}) \int_{T_2}^{T_3} C_{pa} dT}{\eta_{hfo} \times \eta_{rec.}} \quad (17)$$

where $\eta_{rec.}=0.82$ (Heller *et al.* 2006) and $\eta_{hfo}=0.90$ (Xu *et al.* 2011).

Overall thermal efficiency (of power generation) of the combined cycle is given by

$$\eta_{th,ovrl} = \frac{(P_{net})_{GT} + (P_{net})_{ST}}{Q} \quad (18)$$

3.1.4 Process heater

Final temperature of air at the outlet of air mixing chamber is found out. For the process steam supply, the HRSG is assumed to receive saturated water at the supply line pressure of 1.01325 bar and converts it into dry saturated steam at the same pressure. Mass flow rate of steam in the process heater is calculated from the below relationship

$$m_{w_process} = \frac{(m_a + m_{a(Addl.)}) \int_{400}^{T_{Final}} C_{pa} dT}{h_{fg(1.01325)}} \quad (19)$$

3.2 Exergy analysis

In thermodynamics, the exergy of a system is the maximum useful work possible during a process that brings the system into equilibrium with a heat reservoir generally surroundings, considered as the datum state $p_0=1.01325$ bar and $T_0=298$ K. Exergy analysis is the combination of the first and second law of thermodynamics and is defined (Kotas 1985) as the maximum amount of work potential of a material or a form of energy in relation to the surrounding environment. Therefore, exergy analysis points out the losses during a process. The losses are due to (Talbi and Agnew 2000):

- friction
- heat transfer under temperature difference.
- unrestricted expansion.

The total exergy (X_{total}) for a steady flow stream, is the sum of its component exergies, i.e.: physical exergy (X_{ph}), chemical exergy (X_{ch}), kinetic exergy (X_{kin}) and potential exergy (X_{pot}).

$$X_{total} = X_{ph} + X_{ch} + X_{kin} + X_{pot} \quad (20)$$

Neglecting the chemical, kinetic and potential exergy, physical exergy for a given stream can be expressed as (Ghosh and De 2004).

$$X = m \int_{T_0}^T Cp dT - mT_0 \int_{S_0}^S dS \quad (21)$$

The exergy loss in each component is calculated by (Talbi and Agnew 2000)

$$\Delta X = \sum m_i X_i - \sum m_E X_E - Q(1 - \frac{T_0}{T}) - W \quad (22)$$

Exergetic efficiency of a component is given by

$$X_{eff.} = \frac{\sum m_i X_i - \Delta X}{\sum m_i X_i} \quad (23)$$

3.2.1 Exergy analysis of heliostat sub-system

If X_Q is the incident solar radiation exergy and the $X_{rec.}$ is the exergy delivered to the receiver, then the exergy balance for the heliostat sub-system is given by

$$X_Q = X_{rec.} + \Delta X_{helio.} \quad (24)$$

where

$$X_Q = Q(1 - \frac{T_0}{T_{sun}}) \quad (25)$$

T_{sun} is the surface temperature of sun, which has been considered as 5800 K.

Exergetic efficiency of heliostat sub-system is given by the following equation

$$(X_{eff.})_{helio} = \frac{X_{rec.}}{X_Q} \quad (26)$$

3.2.2 Exergy analysis of solar receiver sub-system

The exergy balance of solar receiver sub-system is given by

$$X_2 + X_{rec.} = X_3 + \Delta X_{rec.} \quad (27)$$

where, X_2 and X_3 represent exergy associated with incoming and outgoing air streams for the receiver, $X_{rec.}$ is the solar exergy delivered to the receiver and $\Delta X_{rec.}$ is the exergy destruction for the receiver.

Exergetic efficiency of the solar receiver is given by

$$(X_{eff.})_{rec.} = \frac{X_2 + X_{rec.} - \Delta X_{rec.}}{X_2 + X_{rec.}} \quad (28)$$

In the similar way, exergy destruction and exergetic efficiency of the other sub-systems can be calculated.

4. Discussion on simulated performance of the plant

A custom made program on “C” language has been developed on the basis of the thermodynamic models of the plant components with respect to both the first law and the second law, as described above. The component model was suitably integrated to simulate the overall performance of the CHP plant under varying pressure ratio conditions of the compressor. The basic objective of the present work is to study the performance variations of the solar powered combined heat and power plant (CHP) under varying pressure ratios. The results of the analysis of the plant performance under varying pressure ratios are presented as follows.

This section first describes the base case performance at pressure ratio 5; subsequently, the parametric analyses based on energetic and exergetic performance of the CHP plant at varying pressure ratios of the compressor have been discussed.

The base case performance of the solar powered gas turbine combined cycle power plant is shown in Table 2 at compressor pressure ratio of 5. At the topping cycle (GT) pressure ratio of 5, the plant delivers a net power of 2.37 MW while GT shares a load of 1.90 MW and the balance is supplied by ST. To generate this power, the plant is required to absorb solar power of about 9 MW

Table 2 Base case performance of the solar powered CHP plant

Parameter	Unit	Value
Gas turbine pressure ratio	--	5
Required solar insolation	[MW]	9
GT power	[MW]	1.90
GT cycle thermal efficiency	[%]	21.8
Mass flow rate of steam	[kg/hr.]	1629
Required salt storage	[kg]	46646
Net plant output (GT+ST)	[MW]	2.37
Overall thermal efficiency (power)	[%]	27.14
Heat to power ratio	[-]	0.33

which is equivalent to about 11250 sq. m of collector surface exposed to an average insolation level of 800 W/m^2 .

4.1 Parametric analysis based on energetic performance

The parametric analysis has been carried out at varying pressure ratios of the compressor to find out the energetic as well as exergetic performance of the CHP plant. The pressure ratio has been varied from 4 to 20.

From Fig. 3, it is evident that air temperature at gas turbine exit is decreasing with the increase of pressure ratio. For the combined cycle, since the pinch point temperature difference is set at minimum 15°C for better heat transfer and temperature after gas turbine expansion is decreasing with the increase of pressure ratio, the evaporation rate for the HRSG is decreasing with the increase in pressure ratio. Since the mass flow rate of water is decreasing with the increase of pressure ratio, power obtained from steam turbine is decreasing with the increase of pressure ratio.

It is evident from Fig. 4 that the net power obtained from the gas turbine cycle initially increases; takes a maximum value 1.96 MW at pressure ratio 7 and then decreases with the increase of pressure ratio. For the steam turbine cycle, power obtained from the cycle gradually decreases with the increase of pressure ratio as explained in Fig. 3. Since the gas turbine power takes the major share in the total power obtained from the combined cycle, the total power obtained from the combined cycle also takes initially the upward trend and then a downward trend with the increase of pressure ratio, which is shown in Fig. 4. Fig. 4 also shows the variation of thermal efficiency of gas turbine and combined cycle with pressure ratio. For the gas turbine, thermal efficiency increases with the increase of pressure ratio. But for the combined cycle, overall thermal efficiency increases initially but decreases for the higher pressure ratios since total power obtained from the combined cycle initially increases and then reduces significantly at higher pressure ratios.

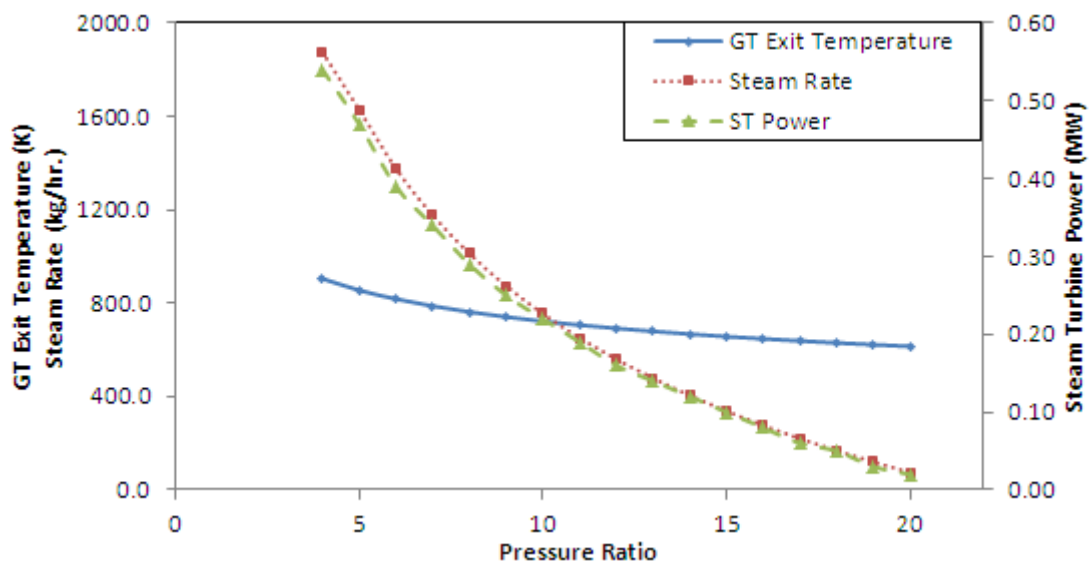


Fig. 3 Variation of GT exit temp., steam rate and ST power with pressure ratio

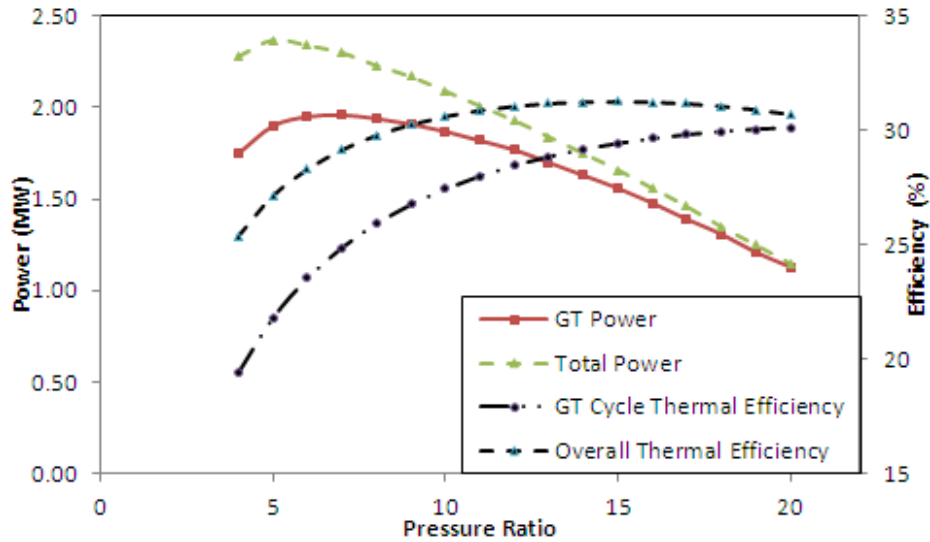


Fig. 4 Variation of GT power, total power, GT cycle and combined cycle thermal efficiency with pressure ratio

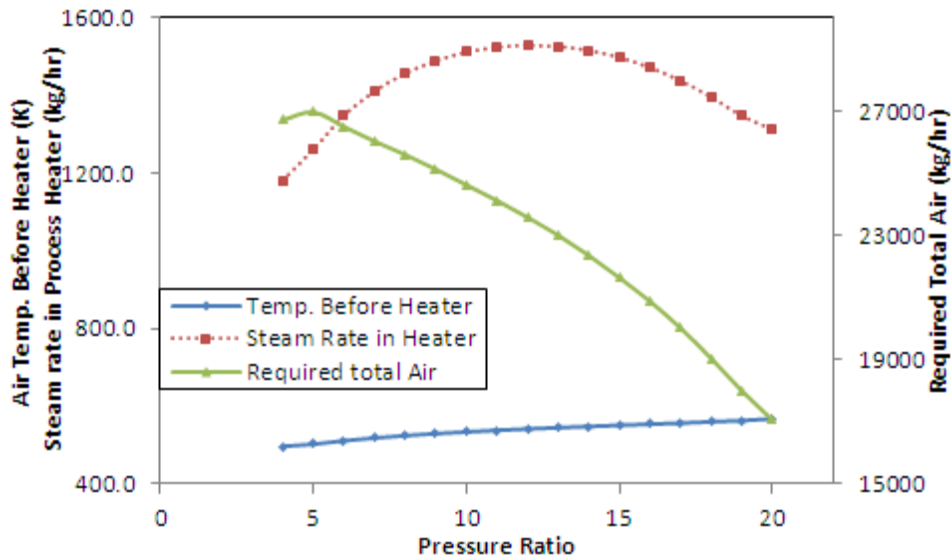


Fig. 5 Variation of air temperature before heater, required total air and steam rate in process heater with pressure ratio

Air from HX1 and HRSG are mixed in the air mixing chamber. This hot air is ultimately used for generating the process steam in the process heater. The temperature of air coming out from the air mixing chamber is increasing with the increase of pressure ratio and the requirement of total air initially increases and then decreases. The combined effect of this is that steam rate in the process heater initially increases; reaches a maximum value at pressure ratio 12 and then decreases with the increase of pressure ratios as shown in Fig. 5.

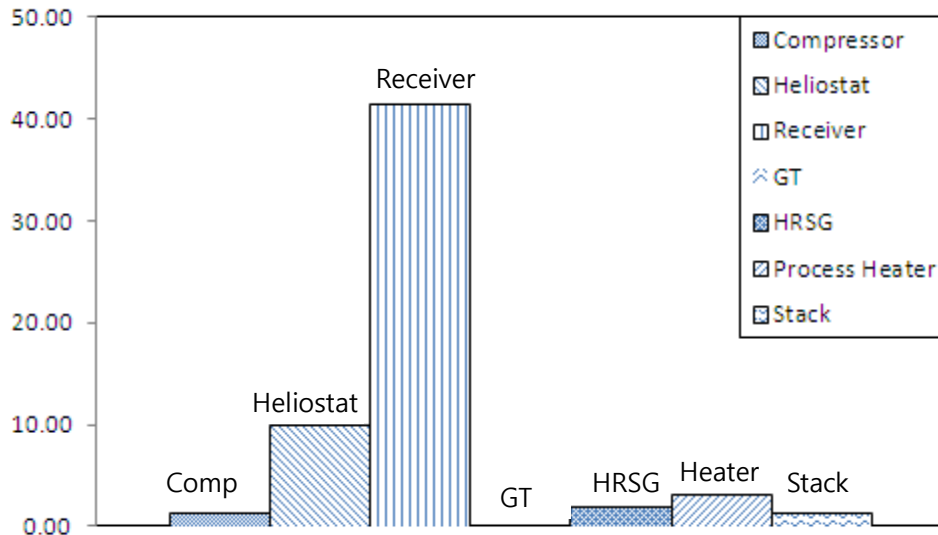


Fig. 6 % Exergy destruction of different components at pressure ratio 4

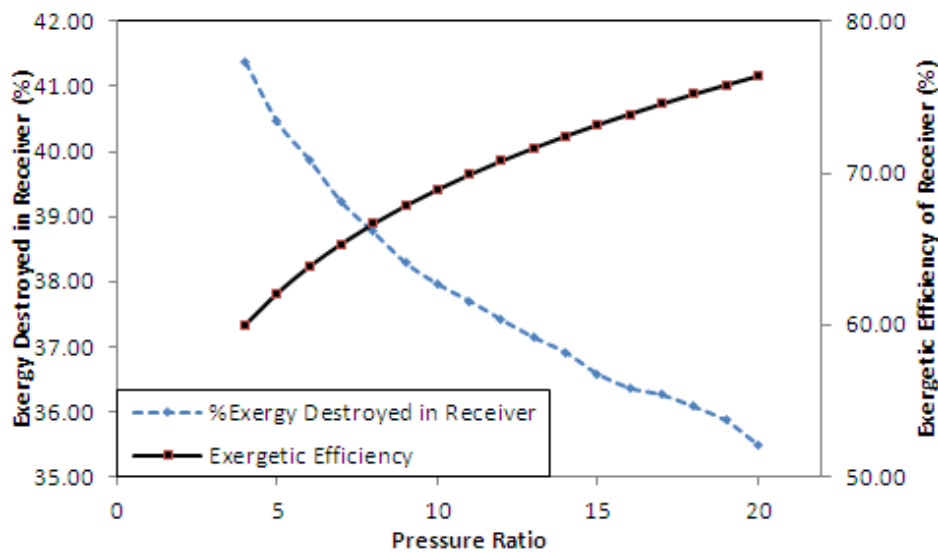


Fig. 7 Variation of exergy destroyed and exergetic efficiency of solar receiver with pressure ratio

4.1 Parametric analysis based on exergetic performance

By exergy analysis, irreversibility or the inefficiency of a process is found out. Fig. 6 shows the lost exergy for different components (compressor, heliostat, solar receiver, gas turbine, HRSG, process heater) and the stack loss for the conceptualized plant (at pressure ratio of 4). Exergy destroyed of a particular component has been calculated with respect to solar exergy input. It is evident from the figure that exergy destruction is the highest for solar receiver, followed by the heliostat and the process heater. High exergy loss of the receiver is because of heat transfer across

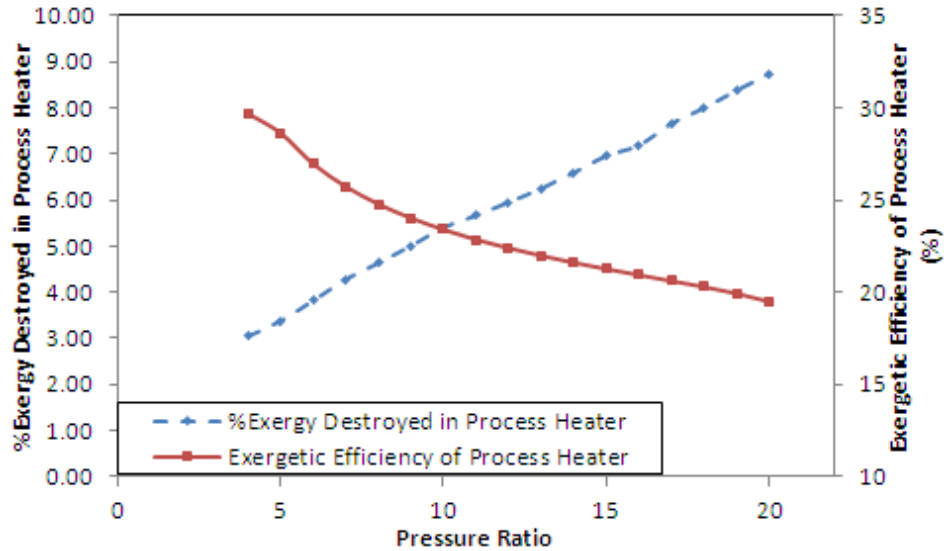


Fig. 8 Variation of exergy destroyed and exergetic efficiency of process heater with pressure ratio

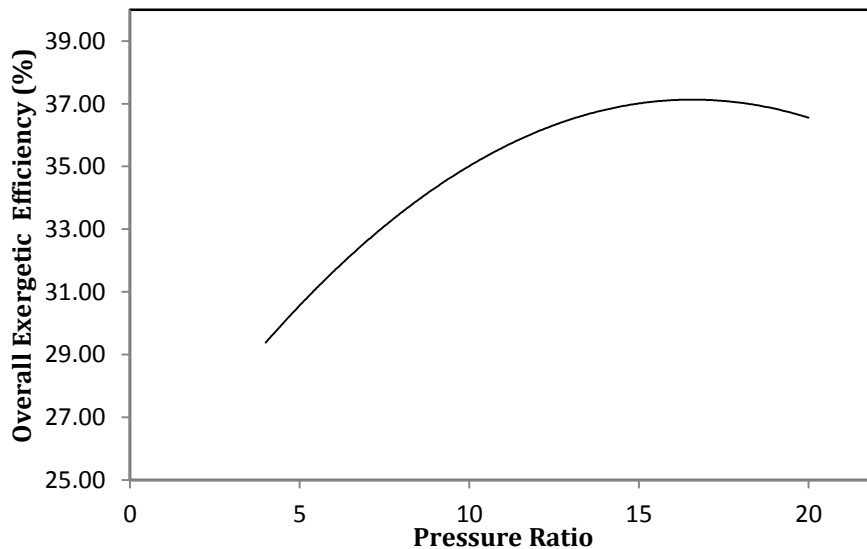


Fig. 9 Variation of exergetic efficiency of the plant with pressure ratio

high temperature difference. In the following sections, parametric analysis of exergy destruction and exergetic efficiency are shown for solar receiver and process heater. Heliostat loss simply represents its optical efficiency and is understandably unaffected by plant parameters.

Fig. 7 shows the variation of exergy destroyed and exergetic efficiency of solar receiver with pressure ratio. While the exergy destruction in the solar receiver shows a decreasing trend, the exergetic efficiency shows an increasing trend. The decrease in exergy destruction with increased pressure ratio is due to the fact that required rate of solar insolation is reducing with the increase of

pressure ratio, resulting in decrease in associated exergy. The required rate of solar energy goes on decreasing with the increase of pressure ratio since temperature of air after compression increases and the gas turbine inlet temperature is fixed at 1000°C. Since the exergy destruction is reducing with the increase in pressure ratio, exergetic efficiency of the solar receiver is increasing with the increase in pressure ratio.

Fig. 8 shows the variation of exergy destroyed and exergetic efficiency of process heater with pressure ratio. Considerable decrease in input solar exergy has been observed with the increase in pressure ratio since rate of solar energy decreases with the increase in pressure ratio as explained earlier. Since percentage exergy destroyed of process heater has been calculated with respect to solar exergy input and input solar exergy is reducing considerably with increase in compressor pressure ratio, exergy destruction in the process heater shows an increasing trend, while the exergetic efficiency shows a decreasing trend.

Fig. 9 shows the variation of overall exergetic efficiency of combined heat and power system with pressure ratio. The overall exergetic efficiency curve is almost similar in nature with overall thermal efficiency curve. It initially increases, reaches a maximum value at about 17 and then decreases with further increase of pressure ratio.

5. Conclusions

A computer program has been developed to predict the performance of a solar power tower combined heat and power cycle. The present study proposes a conceptual configuration of solar tower combined cycle plant with molten salt storage: topping GT cycle with air as the working fluid and a bottoming HRSG plant. The hot molten salt is utilized to produce steam for 4 hours while sufficient sunlight is not available. Below conclusions are drawn from the study.

- One of the biggest challenges for the solar thermal electricity is the intermittency of the solar resource, which can be overcome by incorporating thermal energy storage (TES). Thermal energy storage systems can store the energy during sunshine hours in order to discharge it in a later time i.e., during non-sunshine hours or during cloudy weather condition. Hence, the operation of a solar thermal power plant can be extended beyond the periods of no solar radiation without the need of burning fossil fuels. Thus, energy storage increases the reliability of the concentrated solar thermal power plant. By extending the hours of usage of the power block beyond the sunshine hours, a TES system can reduce the Levelized Cost of Energy (LCOE) for the plant.
- Parametric analysis of the combined cycle has been done for the varying pressure ratio of the compressor and fixed gas turbine inlet temperature. It suggests that power output from combined cycle increases initially, reaches a maximum value (2.37 MW) at pressure ratio of 5 and then decreases. Maximum process heat is obtained at a pressure ratio of 12. The overall thermal efficiency and the overall exergetic efficiency of the combined heat and power system maximises at pressure ratios 15 and 17 respectively. But at higher pressure ratios, power output reduces considerably.
- The exhaust air coming after heating water and the molten salt is having sufficient exergy, which has been utilized to produce process steam.
- Exergetic analysis shows that sufficient exergy is destroyed in solar receiver. The other components where sufficient exergy is destroyed are heliostat, HRSG, stack and process heater.

References

- Cengel, Y.A. and Boles, M.A. (2003), *Thermodynamics An Engineering Approach*, Tata McGraw-Hill Publishing Company Limited, New Delhi, India.
- Flueckiger, S.M., Yang, Z. and Garimella, S.V. (2013), “Review of molten-salt thermocline tank modeling for solar thermal energy storage”, *Heat Transf. Eng.*, 34(10), 787-800.
- Flueckiger, S.M., Iverson, B.D., Garimella, S.V. and Pacheco, J.E. (2014), “System-level simulation of a solar power tower plant with thermocline thermal energy storage”, *Appl. Energy*, 113, 86-96.
- Ghosh, S. and De, S. (2004), “First and second law performance variations of a coal gasification fuel-cell-based combined cogeneration plant with varying load”, *Proceedings of the Institution of Mechanical Engineers, Part A: Journal of Power and Energy*, **218**, 477-485.
- Heller, P., Pfander, M., Denk, T., Felix, T., Valverde, A., Fernandez, J. and Ring, A. (2006), “Test and evaluation of a solar powered gas turbine system”, *Solar Energy*, **80**, 1225-1230.
- Mills, D. (2004), “Advances in solar thermal electricity technology”, *Solar Energy*, **76**, 19-31.
- Montes, M.J., Abanades, A. and Martínez-Val, J.M. (2010), “Thermofluidynamic model and comparative analysis of parabolic trough collectors using oil, water/steam, or molten salt as heat transfer fluids”, *J. Solar Energy Eng.*, **132**, DOI: 10.1115/1.4001399.
- Reuss, M., Beck, M. and Muller, J.P. (1997), “Design of a seasonal thermal energy storage in the ground”, *Solar Energy*, **59**(4-6), 247-257.
- Shabgard, H., Robak, C.W., Bergman, T.L. and Faghri, A. (2012), “Heat transfer and exergy analysis of cascaded latent heat storage with gravity-assisted heat pipes for concentrating solar power applications”, *Solar Energy*, **86**, 816-830.
- Talbi, M.M. and Agnew, B. (2000), “Exergy analysis: an absorption refrigerator using lithium bromide and water as the working fluids”, *Appl. Therm. Eng.*, **20**, 619-630.
- Xu, E., Yu, Q., Wang, Z. and Tang, C. (2011), “Modeling and simulation of 1 MW DAHAN solar thermal power tower plant”, *Renew. Energy*, **36**, 848-857.
- Kotas, T.J. (1985), *The Exergy Method of Thermal Plant Analysis*, Elsevier Ltd.
- Sukhatme, S.P. and Nayak, J.K. (2008), *Solar Energy Principles Of Thermal Collection And Storage*, Tata McGraw-Hill Publishing Company Limited, New Delhi, India.
- European Commission (EC) (2002), SOLGATE Solar hybrid gas turbine electric power system - final publishable report, Publication office, European commission contract ENK5-CT-2000-00333, http://ec.europa.eu/research/energy/pdf/solgate_en.pdf.
- Earth's Energy Budget. <https://ag.tennessee.edu/solar/Pages/What%20Is%20Solar%20Energy/Earth-Energy-Budget.aspx>.
- Herrmann, U., Geyer, M., Kearney, D. (2002), “Overview on thermal storage systems”, *Workshop on Thermal Storage for Trough Power Systems*, http://www.nrel.gov/csp/troughnet/pdfs/uh_storage_overview_ws030320.pdf.
- Kearney, D., Kelly, B., Cable, R., Potrovitza, N., Herrmann, U., Nava, P., Mahoney, R., Pacheco, J., Blake, D. and Price, H. (2003), “Overview on use of a molten salt HTF in a trough solar field”, *NREL Parabolic Trough Thermal Energy Storage Workshop*, <http://www.nrel.gov/csp/troughnet/pdfs/40028.pdf>.
- Solar Server Report: Abengoa Yield's Mojave 280 MW CSP plant declares commercial operation. <http://www.solarserver.com/solar-magazine/solar-news/current/2014/kw49/abengoa-yields-mojave-280-mw-csp-plant-declares-commercial-operation.html>.

Nomenclature

T	[K]	Temperature	Special Characters	
r	[-]	Pressure ratio	η	[-] Efficiency
k	[-]	Ratio of specific heats	Subscripts	
m	[kg/s]	Mass	e	[-] Expansion
P	[MW]	Power	GT	[-] Gas Turbine
h	[MJ/kg]	Enthalpy	ST	[-] Steam Turbine
HX	--	Heat Exchanger	C	[-] Compression
M	[kg]	Mass of salt	w	[-] Water/Steam
X	[MW]	Exergy	a	[-] Air
S	[MJ/K]	Entropy	A, B, C, \dots	[-] State Points
W	[MJ]	Work	$mech$	[-] Mechanical
Q	[MJ]	Solar insolation	G	[-] Generator
th	[-]	Thermal		
1, 2, 3..	[-]	State Points		
Addl.	[-]	Additional		
hfo.	[-]	Heliostat field optic Eff.		
rec.	[-]	Receiver		
0	[-]	Dead state		
i	[-]	Inlet		
E	[-]	Exit		